

Deciphering “cryptic” nature of European rock-dwelling *Pyramidula* snails (Gastropoda: Stylommatophora)

Veronika Horskáková | ORCID: 0000-0002-3264-7728

Department of Botany and Zoology, Faculty of Science, Masaryk University, Brno 61137,
Czech Republic
veronika.horskakova@seznam.cz

Eva Líznarová

Department of Botany and Zoology, Faculty of Science, Masaryk University, Brno 61137,
Czech Republic

Oihana Razkin

Department of Zoology and Animal Cell Biology, University of the Basque Country
(UPV/EHU), 01006 Vitoria-Gasteiz, Spain

Jeffrey C. Nekola

Department of Botany and Zoology, Faculty of Science, Masaryk University, Brno 61137,
Czech Republic

Michal Horskák

Department of Botany and Zoology, Faculty of Science, Masaryk University, Brno 61137,
Czech Republic

RECEIVED: 7 JANUARY 2022 | REVISED AND ACCEPTED: 11 APRIL 2022; PUBLISHED ONLINE:
23 MAY 2022; PUBLISHED IN ISSUE: 26 AUGUST 2022

EDITOR: T. DE WINTER

Abstract

Many molecular phylogenetic studies conclude by reporting discoveries of new “cryptic” species. However, these putative biological entities are typically left unverified outside of the DNA evidence or subjected to only superficial *post-hoc* analyses. Minute land snails of the Western Palearctic *Pyramidula* represent one of such examples being considered a cryptic species complex based on previously conducted molecular phylogeny. Several species appear indistinguishable due to noticeable shell tendency towards either

high-spired (*Pyramidula rupestris* and *P. jaenensis*) or low-spired (*P. saxatilis* and *P. pusilla*) morphotype. Here, we challenge this conclusion by using mtDNA, nDNA, morphometric analyses and qualitative shell features, and seek for a potential evolutionary mechanism behind the conchological similarities. Through an empirical integration of multiple data types we document that the studied taxa can be visually distinguished. Unlike isolated shell measurements, CVAs based on traditional morphometrics and geometric morphometrics have power to separate all species from each other, except for *P. saxatilis* and *P. pusilla*. However, only a use of previously overlooked shell surface microsculpture makes it possible to identify individuals of all species. Considering tight associations between shell measurements and climate, we propose an evolutionary explanation based on optimization of thermal flux under different climatic selection pressures. Our study brings the awareness towards microscopic shell features, and outlines a general protocol to identify robust visual identification criteria in taxonomic groups containing cryptic (and non-cryptic) members. It also exemplifies an integration of various data types for macroscale species identification, which we believe should follow any discovery of putatively cryptic species.

Keywords

cryptic species – integrative taxonomy – landmarks – microsculpture – multivariate morphometrics – *Pyramidula*

Introduction

Cryptic species are phylogenetically distinct taxonomic units which appear so similar in standard morphological / anatomical / ecological / behavioral traits that they have been grouped under a single taxonomic name (Bickford et al., 2007; Schlesinger et al., 2018; Struck et al., 2018). However, many putative cryptic species have thus far only been assessed from a single source of genetic data, typically mitochondrial DNA, despite clear limitations of this approach (e.g., Rubinoff et al., 2006; Wiens et al., 2010). Well-documented is the higher rate of spatial-structuring seen in mitochondrial as compared to nuclear DNA due to its matrilineal-only transmission with no recombination leading to a greater incidence of taxonomically-uninformative clustering (e.g., Nekola et al., 2015). Although some authors suggest that any single line of well-supported evidence is sufficient to

document a cryptic species (e.g., Valdecasas et al., 2008; Padial et al., 2010; Jörger & Schrödl, 2013; Fišer et al., 2018), this concept seems incongruous with evolutionary theory: because species separation is ultimately related to gene flow interruption, at least some macro-scale feature must exist to initiate isolation. And after species have become independent evolutionary units and begin taking their own separate trajectories (e.g., Mayden, 1997; Mayr, 2000), natural selection and neutral process should lead to the gradual accumulation of unique traits (De Queiroz, 2007). Cryptic species hypotheses thus can (and should) be subjected to the same integrative empirical confrontation (e.g., Dayrat, 2005; Will et al., 2005; Schlick-Steiner et al., 2010) used for “non-cryptic” species. That is – being proposed with respect to a particular species concept (e.g., Baker & Bradley, 2006; Fišer et al., 2018) – they are accepted only after a consensus for divergence is achieved across

multiple data sources (e.g., Padial et al., 2010; Schlesinger et al., 2018; Hinojosa et al., 2019; Horsáková et al., 2019). Because almost all presumed “cryptic” species-level clades can actually be distinguished by at least some macroscale traits (e.g., Sáez & Lozano, 2005; Schlick-Steiner et al., 2007; Tan et al., 2010; Schlesinger et al., 2018; Horsáková et al., 2019), crypticity may potentially say more about limits of traditional taxonomic observation than biology (Karanovic et al., 2016; Heethoff, 2018).

In this work we exemplify an integration of multiple information channels in search for robust macroscale species identification, which we believe should follow any discovery of putative cryptic species. For that purpose, we focus on the Western Palearctic members of the land genus *Pyramidula* Fitzinger, 1833, which has been recently subjected to robust phylogenetic analyses. Specifically, we examine two species of high-spined morphotype, i.e., *P. rupestris* (Draparnaud, 1801) and *P. jaenensis* (Clessin, 1882), and two of low-spined morphotype, i.e., *P. pusilla* (Vallot, 1801) and *P. saxatilis* (Hartmann, 1842). Due to high intraspecific variation and profound similarity in observable and easy-to-measure conchological features, they have been considered to represent a cryptic species complex (Razkin et al., 2016, 2017). We investigate this conclusion through an integrative empirical confrontation across mtDNA sequence, nDNA sequence, quantitative analyses (traditional multivariate morphometrics, and geometric morphometrics) and qualitative shell data as well as ecological preference, biogeography, and climate niche data. Our main goals are to (i) verify putative morphological crypticity of the four study species; (ii) seek for potential evolutionary processes / mechanisms which may underlie identified shell form similarities; (iii) rectify the nomenclature of the study system; and (iv) detail the best practices which should be used in empirically-driven

integrative taxonomic revisions of “cryptic” (and other) species groups.

Material and methods

Study system

Pyramidula possesses minute (<3 mm height and diameter), dome-shaped or conical shells with an open umbilicus, simple aperture, and yellowish grey to dark brown color (Kerney & Cameron, 1979; Gittenberger & Bank, 1996). They are restricted to base-rich rock surfaces (Klemm, 1974) and occur across a wide range of climates and altitudes (Welter-Schultes, 2012; Schileyko & Balashov, 2012) ranging from Western Europe across Central Asia to Japan (Pilsbry & Hirase, 1902; Balashov & Gural-Sverlova, 2011; Welter-Schultes, 2012). In Europe, six nominal species are currently accepted (Gittenberger & Bank, 1996; Razkin et al., 2017), i.e., *P. cephalonica* (Westerlund, 1898), *P. chorismenostoma* (Blanc, 1879), *P. jaenensis*, *P. pusilla*, *P. rupestris*, and *P. saxatilis*. In Asia, additional species occur but their taxonomy has not yet been fully resolved (Balashov & Gural-Sverlova, 2011; Razkin et al., 2017). As noted for other minute land snails (e.g., Pokryszko et al., 2009), their genitalic anatomy is simple (Martínez-Ortí et al., 2007) and therefore unlikely to bear species-specific features. Species diagnoses in the group have thus long relied only on conchological characters (Gittenberger & Bank, 1996). While a number of Western European species have been erected since the 19th century, until the mid-1990s all had been synonymized into *P. rupestris*. Gittenberger & Bank (1996) questioned this approach and concluded that at least six species were actually present in Europe. However, their diagnostic characters and biogeographic ranges remained unresolved (Welter-Schultes, 2012). These issues were partially addressed by Razkin et al. (2016,

2017) who confirmed existence of nine genetically well-supported species in the Western Palearctic realm based on both nDNA and mtDNA sequence. However, for several of them variation in basic shell morphology largely overlapped. This was also the case of four species commonly (and often sympatrically) occurring in temperate Europe and adjacent Iberian and Apennine Peninsulas, i.e., *P. jaenensis*, *P. pusilla*, *P. rupestris*, and *P. saxatilis*. *Pyramidula pusilla* and *P. saxatilis* typically have low conical, broader-than-high shells with relatively wide umbilicus, while *P. rupestris* and *P. jaenensis* have high conical, usually higher-than-broad shells with relatively narrow umbilicus (Gittenberger & Bank, 1996; Razkin et al., 2017). Based on the analysis of landmarks, a distinction in shell form between *P. jaenensis* and *P. rupestris*, along with trends in radular microstructure, have been pointed out by Miller et al. (2021). However, this distinction was based on a small number of populations from Spain, not accounting for the variation across the full geographic ranges of the species. Therefore, as of now, these species lack diagnostic shell characters and require DNA data for accurate identification.

Considering the complexity and robustness of evidence that is necessary to evaluate potential morphological crypticity within *Pyramidula*, we limit ourselves to the four common and most difficult-to-distinguish European species. Further studies are needed to target other members of the genus, including undescribed candidate species suggested by Razkin et al. (2016, 2017).

Initial specimen selection

For initial genetic analyses, we assembled a representative set of 35 populations identified as *P. jaenensis*, *P. pusilla*, *P. rupestris* or

P. saxatilis, aiming to include ~ 7–10 specimens from distinct sites per species. Because no unambiguous diagnostic criteria had been defined for these species, we were only able to conduct preliminary taxonomic assignments based on morphological descriptions reported in Gittenberger & Bank (1996) and Razkin et al. (2017). As a main guidance, however, we used available data on genetically verified populations. For *P. jaenensis* and *P. rupestris* we mostly selected specimens from populations analyzed by Razkin et al. (2016, 2017). For *P. saxatilis* we used newly collected material from regions with its confirmed occurrence (mainly the Alps), while for *P. pusilla* we used material from regions with its confirmed occurrence, but without reported *P. saxatilis* (mainly temperate lowlands and the Carpathians). The new material was collected by the authors in 2008–2020 (two samples were collected by R. Coufal in 2020). Samples were selected to cover the Central European and North Mediterranean extent of each species range (fig. 1; supplementary table S1), with a particular focus being placed on *P. saxatilis* which was under-represented in Razkin et al. (2016, 2017). In addition, we were able to extract DNA from an individual included in a large *P. saxatilis* type series courtesy of curator Dr. K. Urfer.

DNA extraction, PCR and sequence analysis

Tissue samples were either preserved in absolute ethanol or allowed to mummify at ambient temperature and humidity. DNA was extracted using the E.Z.N.A. Mollusc DNA Kit (Omega BioTek) and stored at -20°C . All shells were microscopically imaged prior to extraction using standard protocols (Nekola et al., 2009, 2018). PCR amplification was performed for one mitochondrial (cytochrome oxidase subunit 1 – CO1) and two linked

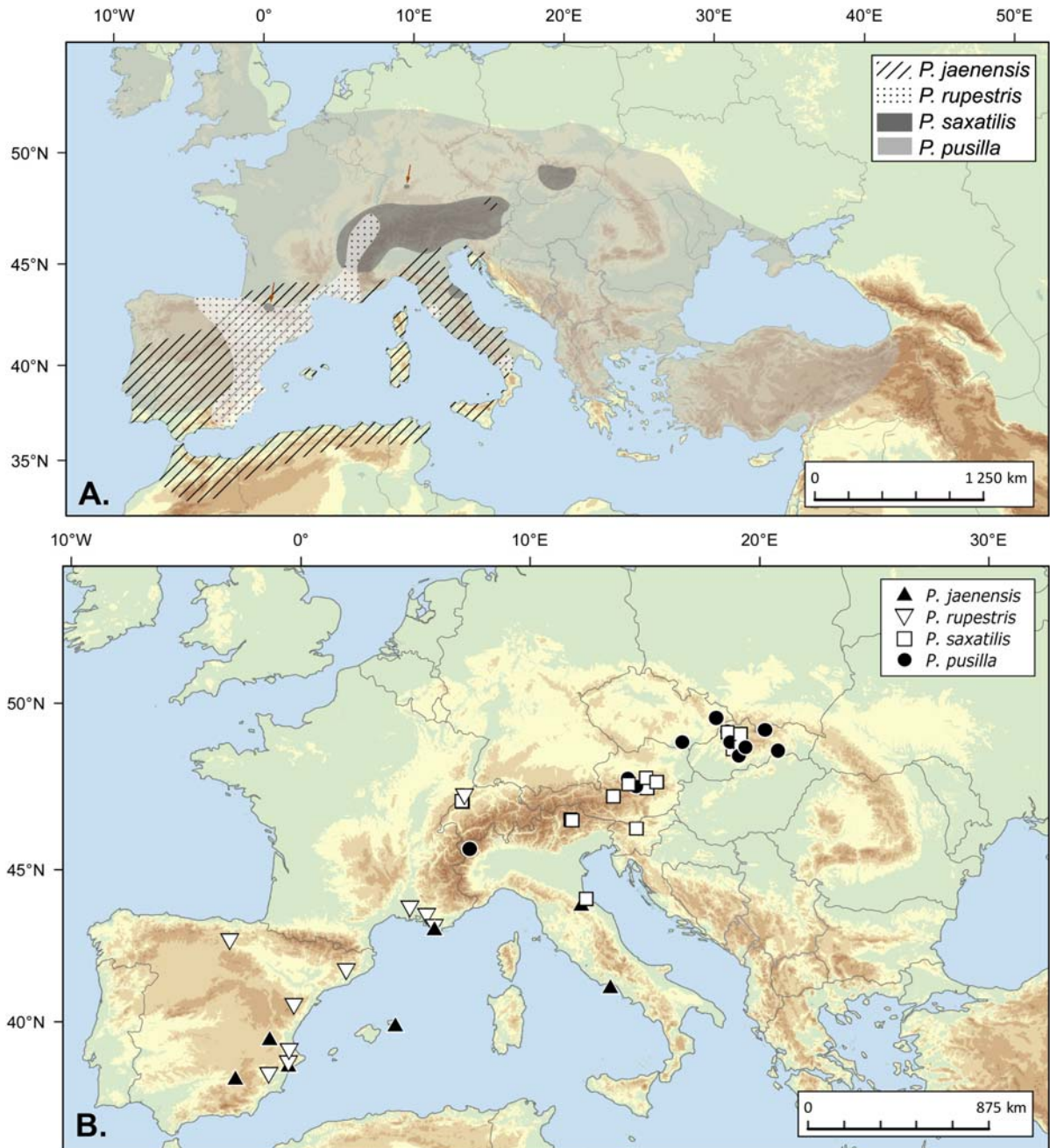


FIGURE 1 A. Approximate distribution of the four study species based on genetically verified data in the present study and integrative analysis of Razkin et al. (2017). B. Geographic location of all genetically analyzed *Pyramidula* populations. Detailed information about the localities are shown in supplementary table S1.

nuclear loci (internal transcribed spacers ITS1 and ITS2). Primer sequences are listed in table 1. PCR mix consisted of 12.5 μ l PCR Mastermix, 1 μ l of each primer (10 pmol), 8.5 ddH₂O and 2 μ l genomic DNA. Cycling conditions for PCR amplification were as follows: 10 min at 96°C

[30 s at 94°C, 30 s at 45°C (COI) or 52°C (ITS), 1 min at 72°C] \times 40 cycles, and 10 min at 72°C. PCR products were purified using ExoSAP (Affymetrix) and cycle sequenced at OMICS Core facility or SEQme s.r.o. Forward and reverse strands were assembled in Geneious

TABLE 1 Primer sequences for genetic markers COI, ITS1 and ITS2, authors of primer design, and anneal temperatures (°C) used for PCR amplification

Region	Name	Sequence	Author	Anneal T (°C)
COI (F)	LCO1490	5'-AAATAATGCTATTTTCATGAYCAYGC-3'	Folmer et al. (1994)	45
COI (R)	HCO 2198	5'-GCTCCGCAAATCTCTGARCAYTG-3'	Folmer et al. (1994)	45
ITS1 (F)	18S rDNA	5'-TAACAAGGTTTCCGTATGTGAA-3'	Armbruster & Bernhard (2000)	52
ITS1 (R)	LSU1rc	5'-TCACATTAATTCTCGCAGCTAG-3'	Nekola et al. (2018)	52
ITS2 (F)	LSU-1	5'-CTAGCTGCGAGAATTAATGTGA-3'	Wade & Mordan (2000)	52
ITS2 (R)	LSU3rm	5'-GGTTTCACGTACTCTTGAAC-3'	Nekola et al. (2018)	52

v. 8.0.2 (Biomatter Ltd.) and checked by eye for potential errors. Amino acid translation of the COI fragment was used to check for erroneous stop codons. In the few cases when two bases were equally represented at a given ITS position we applied IUPAC ambiguity codes. GenBank accession numbers for all sequences used in phylogenetic analysis are provided in supplementary table S1. ITS1 and ITS2 were concatenated and aligned with online Mafft v.7 (Kuraku et al., 2013; Katoh et al., 2019) using the Q-INS-i algorithm which considers secondary rRNA structure (Katoh & Toh, 2008). All alignments were visually inspected for potential errors, and are available upon request.

Phylogeny reconstruction

Phylogenetic analyses were performed separately on the COI and ITS1 + 2 constructs. We opt for not concatenating mtDNA and nDNA data because they are known to have different modes of inheritance, mutation rates, and evolutionary histories, and can therefore produce conflicting results (Fisher-Reid & Wiens, 2011; Nekola et al., 2015; Horsáková et al., 2019). To ensure robust and well-supported tree topology, we conducted four different

reconstruction methods, each based on very different analytical assumptions: MEGA v.6.0 (Tamura et al., 2013) was used to construct Neighbor-joining (NJ) trees, using maximum composite distance including transitions and transversions with pairwise gap deletion, and Maximum parsimony (MP) trees, using heuristic search with 1000 replicates and TBR branch-swapping algorithm, with gaps being treated as missing data. For the Maximum likelihood (ML) and Bayesian inference (BI), the ITS1 + 2 fragment was partitioned by the two amplicons, with two separate partitions being created for COI based on the 1st + 2nd and 3rd codon positions. ML analysis was performed in RAxML v 8.2 (Stamatakis, 2014), using 500 search replicates and the GTR + G models of sequence evolution for separate gene partitions. Internal node support was assessed via 1000 non-parametric bootstrap replicates (Felsenstein, 1985) for the NJ, MP, and ML analyses. For BI, optimum nucleotide substitution models for each gene partition were selected using jModelTest v. 2.1.10 (Darriba et al., 2012) using the Bayesian Information Criterion. BI was performed in MrBayes v3.2.6 (Huelsenbeck & Ronquist, 2001), simultaneously running one cold and

three heated MCMC chains for 10 000 000 generations, sampling every 1000 generations and with a burn-in of 25%. We ran four independent searches and used Tracer 1.6 (Drummond & Rambaut, 2007) to assess convergence, checking that the effective sample sizes of all parameters were higher than 200 and standard deviation of split frequencies lower than 0.01. Only support values above 70 for NJ, MP, and ML, and posterior probabilities above 95 for BI are shown in the final trees. Because tree topologies were essentially identical between all four methods, ML trees were used to visualize phylogeny via the Interactive Tree Of Life v.5.7 annotator (Letunic & Bork, 2021). The analyses are midpoint rooted due to impossibility to align the ITS1 + ITS2 fragment with that of any taxon outside of the genus *Pyramidula* (see also Nekola et al., 2018).

Genetically validated species were considered present when they possessed highly supported reciprocally-monophyletic clades in both the nDNA and mtDNA across a consensus of reconstruction methods.

Validation of qualitative shell features

After the initial phylogenetic analysis, we examined additional specimens from the genetically verified populations, to search for a suite of consistent diagnostic shell traits that would be shared among members of the same species, but differ from those of the other species. These traits included: shell lustre and color, protoconch and teleoconch surface microsculpture, presence and arrangement of ribs / striae / growth ridges, ridge angle, ridge density per 0.5 mm of teleoconch surface, apex formation, coil expansion, and suture depth. Surface features were imaged using a Keyence VHX-5000 digital microscope with ZS-20 and ZS-200 objective lenses. A special focus was put on the variability of mixed populations, i.e., from localities with sympatric occurrence of more than one species. Genitalic anatomy

was not evaluated as it is known to be simple (Martínez-Ortí et al., 2007; Miller et al., 2021) and therefore unlikely to bear species-specific features, similarly as in other minute land snail species (e.g., Pokryszko et al., 2009).

Once potentially diagnostic traits were targeted, we sequenced and analyzed additional specimens using methods described above, to evaluate stability, consistency, and taxonomic utility of each trait. This iterative procedure enabled us to calibrate intraspecific vs. interspecific morphological variability. We finished the procedure when there was no mismatch between the morphology-based identification using newly targeted traits, and genetic analysis of the data, with a total of 64 genetically analyzed specimens (35 from the initial set, and 29 from the additional analyses).

Shell measurements

From each of the genetically verified populations we selected a representative number of mature specimens ≥ 4 whorls for analysis (supplementary table S1). We were unable to genetically verify all specimens selected for morphometric analyses, because the shell destruction required for DNA extraction would not have left material for subsequent examination of the specimens. In addition, some mature specimens were represented by empty shells or shells with poorly preserved tissue, preventing DNA extraction. However, the newly targeted qualitative species-level traits ensured that all specimens were reliably identified and placed into species-level groups prior to morphometric analyses. The final dataset comprised 55 *P. pusilla* (from 12 populations), 50 *P. saxatilis* (11), 28 *P. rupestris* (9) and 29 *P. jaenensis* (7) individuals. We also acquired type specimen images of *P. pusilla* (neotype, Natural History Museum, Dijon, France, No. 210.996.MO.1, provided by E. Fara); *P. rupestris* (lectotype, Natural History Museum, Vienna, Austria, J. Draparnaud

collection xxvi 97a, provided by I. Gallmetzer, © NHMW), *P. jaenensis* (type series, S. Clessin collection, State Museum of Natural History Stuttgart, Germany, SMNS-ZI0142153, provided by D. Wanke and M. Pallmann, © SMNS), and *P. saxatilis* (type series, J.D.W. Hartmann collection, Natural History Museum St. Gallen, Switzerland, M562, imaged by the authors).

Each measured shell was imaged from top, bottom and front using an Olympus SZX7 microscope with Olympus C-7070 Wide Zoom camera and QuickPHOTO MICRO software to provide Deep Focus. This was accomplished by assembling four to nine sequential stacked in-focus images. The type *P. jaenensis*, *P. pusilla*, *P. rupestris*, and *P. saxatilis* images were also used.

Shell width and height, aperture width and height, body whorl height, and umbilicus width were determined from these images (supplementary fig. S1). The number of whorls was counted according to Cameron (2003). Because shells of this genus are roughly of conical shape, shell volume (v) was estimated via:

$$v = \left(\pi * (Sw / 2)^2 * Sh \right) / 3,$$

where Sw = shell width (mm) and Sh = shell height (mm).

To account for potentially different growth stages of the individuals, we also calculated ratios between measured shell characteristics, i.e., shell width/number of whorls, shell height/number of whorls, shell height/shell width, body whorl height/shell height, aperture width/shell width, aperture width/shell height, aperture height/body whorl height, and umbilicus width/number of whorls.

Traditional and geometric morphometrics

Given their demonstrated utility, both traditional multivariate morphometrics and geometric morphometrics (Karanovic et al., 2016; Horsák & Meng, 2018; Horsáková et al.,

2019) were used to explore whether genetically-verified species differ in morphospace. For the traditional morphometrics, shell measurements and their ratios were visualized by histograms to check for normality prior to analyses, and analyzed via the Canonical Variance Analysis (CVA). Significance was estimated using 10,000 permutations of Mahalanobis (for pooled within-group covariance matrix) and Euclidean (between group means) distances using the “Morpho” package; Schlager, 2017). Measured shell characteristics were linearly fitted into two-dimensional ordination space using the function ‘envfit’ implemented in the ‘vegan’ R package (Oksanen et al., 2017). The fit was tested using 4999 permutations, to identify those shell characteristics that are most informative for species delimitation.

Vector loading of each measured shell characteristic was fit into the two-dimensional ordination space, with importance being estimated using 4999 permutations. For the geometric morphometrics, the coordinates of 16 landmarks were placed on the frontal view of the shell (see supplementary fig. S2 for their position). The data were subjected to a Procrustes superimposition (Gower, 1975) and analyzed using CVA. The analyses were conducted in R 3.5.2 using the ‘ade4’ (Dray & Dufour, 2007), ‘vegan’ (Oksanen et al., 2017), and ‘geomorph’ (Adams et al., 2021) packages.

Climatic variables

A set of climatic variables was compiled for each population using its geographic coordinates, including Thornthwaite Aridity Index (TAI) and 19 Bioclimatic variables (BIO1–BIO19), extracted via the WorldClim v1.4 database (Hijmans et al., 2005) and the Arcgis 8.3 program (ESRI, 2003). The full set of variables was reduced to those that were not strongly correlated with each other (Spearman rho < |0.8|). Relationships between the climatic variables and shell parameters were explored

using Spearman correlations. In the cases of multiple testing, Holm correction was applied to adjust the P-values (Holm, 1979). For the strongest relationships, linear regressions were modelled and tested using the F-statistic to assess significance, and adjusted R^2 to express the percentage of explained variation. Selected strong relationships were visualized via scatterplots. Climatic analyses were conducted in R 3.5.2 using the ‘vegan’ (Oksanen et al., 2017) and ‘ggplot2’ (Wickham, 2016) packages.

Results

Phylogeny reconstruction

A total of 64 individuals are subjected to phylogenetic analysis, including 22 individuals of *P. pusilla* from Austria, Czech Republic, Italy, and Slovakia (from 13 populations); 23 *P. saxatilis* from Austria, Italy, San Marino, Slovakia, and Switzerland (17 populations); 12 of *P. rupestris* from France, Spain, and Switzerland (10 populations); and 7 of *P. jaenensis* from France, Italy, San Marino, and Spain (7 populations; supplementary table S1).

DNA sequence data were obtained from all 64 specimens in COI and from 58 specimens in the ITS1 + 2 construct (fig. 2, supplementary table S1). Total amplicon lengths (trimmed of primer ends) are 655 bp for COI, 605–639 bp for ITS1 and 797–822 bp for ITS2 fragments, with the resultant ITS1 + 2 construct ranging from 1402–1456 bp. The number of variable base pair positions is 148 bp in COI, 39 bp in ITS1, and 56 bp in ITS2. The number of base pair differences within species range from 0.6 to 10.7 in ITS1 + 2, and from 8.6 to 40.1 in COI. Base pair differences between species range from 7.3 to 33.5 in ITS1 + 2 and from 34.8 to 53.4 in COI.

In ITS1 + 2 individuals are sorted into four highly-supported species-level clades (fig. 2), corresponding to *P. pusilla*, *P. saxatilis*,

P. jaenensis, and *P. rupestris*. Three highly supported and reciprocally monophyletic clades representing *P. pusilla*, *P. jaenensis*, and *P. rupestris* are also present in COI, while *P. saxatilis* does not reach high support. Both mtDNA and nDNA phylogenies group *P. pusilla*, *P. rupestris*, and *P. saxatilis*, with *P. jaenensis* being more distant, and document that *P. rupestris* and *P. saxatilis* are sister taxa. Based on these analyses six sympatric occurrences of *P. pusilla* and *P. saxatilis* are noted, two of *P. jaenensis* and *P. rupestris*, and one of *P. jaenensis* and *P. saxatilis*. One individual (P368) possesses nDNA of *P. jaenensis* but mtDNA of *P. rupestris*.

To verify the identification of putative *P. saxatilis* lectotype, we sequenced 603 bp of the COI gene from one individual of this >170 years old material. In the phylogenetic reconstruction based on this marker alone, the individual is genetically identical with some other *P. saxatilis* individuals (supplementary fig. S3).

Traditional morphometrics and landmarks

Descriptive statistics for all shell measurements and their ratios are provided in supplementary table S2. No single quantitative trait (or assorted ratios) is able to unambiguously define genetically verified species-level clades, with all exhibiting considerable variation within and overlap between species (table 2a, supplementary table S2). However, two distinct morphotypes can be observed (fig. 3): the low-spined, wide-umbilicus *P. pusilla* / *saxatilis* (mean height / width ~ 0.7, umbilicus width / no. of whorls ~ 0.18), and high-spined, narrow-umbilicus *P. jaenensis* / *rupestris* (mean height / width ~ 0.95, umbilicus width / no. of whorls ~ 0.12). In spite of this, so much intraspecific variation exists that essentially identical shell shapes can occur across all four species (fig. 3e).

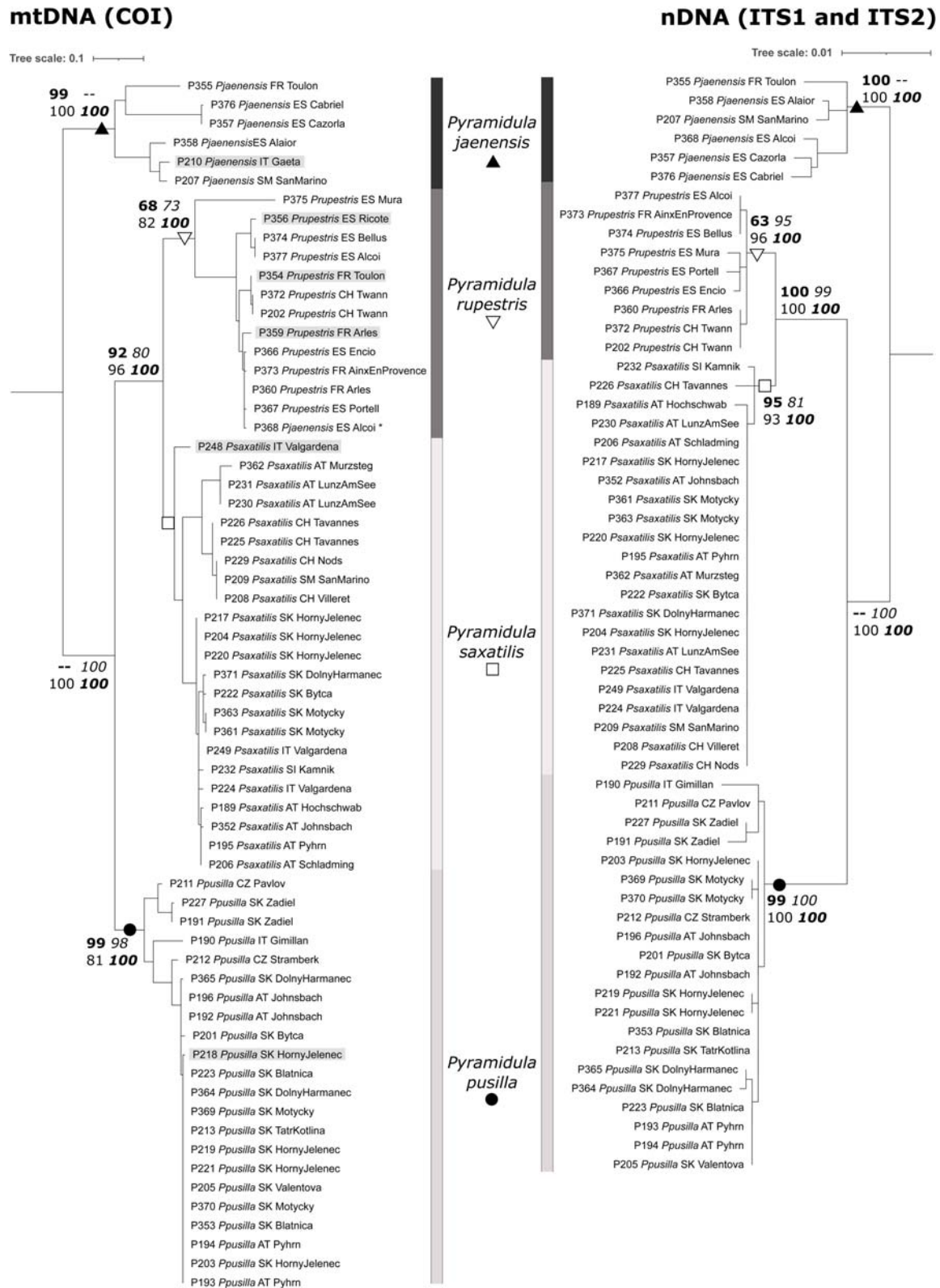


FIGURE 2 Maximum likelihood (ML) phylogenetic reconstruction based on mitochondrial DNA (COI) and nuclear DNA (concatenated ITS1 and ITS2). Support values of > 70% are shown next to the corresponding nodes as follows: NJ, upper left, bold font; MP, upper right, italic font; ML, lower left, normal font, and posterior probabilities of > 95% for BI, lower right, bold italic font. Specimens for which only mtDNA data exist are highlighted in grey color. Specimen placed in a different clade in mtDNA and nDNA is marked by asterisk. Symbols used for each species correspond to those in fig. 1.

TABLE 2 Variation in measured shell characteristics (A) and qualitative conchological features (B) in the studied *Pyramidula* species

A. Shell measurements						
Taxon	Shell width mm (min–max)	Shell height mm (min–max)	Umbilicus width (mm)	Shell width / No. of whorls (min–max)	Shell height / No. of whorls (min–max)	Umbilicus width / No. of whorls (min–max)
<i>P. pusilla</i>	2.12–2.89	1.54–2.15	0.55–1.00	0.49–0.70	0.37–0.51	0.13–0.24
<i>P. saxatilis</i>	2.14–2.82	1.57–2.30	0.52–0.92	0.53–0.70	0.38–0.54	0.12–0.22
<i>P. rupestris</i>	2.08–2.47	1.71–2.65	0.33–0.60	0.46–0.60	0.44–0.65	0.07–0.16
<i>P. jaenensis</i>	1.93–2.73	1.95–2.81	0.39–0.81	0.46–0.68	0.47–0.60	0.09–0.19

B. Qualitative characters				
Taxon	Shell shape	Apex	Coil expansion	Suture formation
<i>P. pusilla</i>	low-spire, broader than wide, wide umbilicus*	blunt	slow	shallow
<i>P. saxatilis</i>	low-spire, broader than wide, wide umbilicus**	blunt	slow to fast (rarely very fast)	shallow
<i>P. rupestris</i>	high-spire, height similar to width, narrow umbilicus***	distinctly pointed	fast or very fast	deep, very tumid whorls
<i>P. jaenensis</i>	high-spire, sometimes very conical, narrow umbilicus****	distinctly pointed	slow	deep, very tumid whorls

Taxon	Color	Lustre	Protoconch structure	Teleoconch structure	Ridge density per 0.5 mm	Angle of growth ridges
<i>P. pusilla</i>	light- to dark red-dish-brown	dull to silky	none	fine, often irregular ridges, anastomose frequent	< 14	> 45°
<i>P. saxatilis</i>	brownish dark (light)	silky to dull	none	dense, very regular thread-like ridges, without anastomose	> 20	> 45°
<i>P. rupestris</i>	dark red-dish-brown	dull to silky	rugged	coarse, irregular to rather regular ridges, anastomose frequent	< 10	< 45°
<i>P. jaenensis</i>	yellowish grey to dark brown	dull	rugged	dense, very regular thread-like ridges, without anastomose	> 14	< 45°

Abbreviations and symbols: *, continuous variation towards very low conical shells with widely open umbilicus (around 0.4 of the shell width); **, some individuals possess relatively high spires compared to typical phenotypes; ***, can occur in two forms: 1 – fast growing with high body whorl, large aperture, very narrow umbilicus, and shiny lustre, 2 – slightly flatter shells with lower body whorl, smaller aperture, wider umbilicus, and somewhat more regular structure of dull appearance; ****, some populations reach nearly scalaroid shape with tilted, pointed apex.

CVA based on traditional morphometrics provides clearer species resolution (table 3, fig. 4). Variation along the first axis is mostly related to shell height / width ($R^2 = 0.87$) and umbilicus width ($R^2 = 0.81$), differentiating *P. jaenensis* / *rupestris* from *P. pusilla* / *saxatilis*. The second axis mainly reflects the number of whorls ($R^2 = 0.33$), differentiating *P. jaenensis* from *P. rupestris*. *Pyramidula pusilla* and *P. saxatilis* overlap almost completely. Overall classification accuracy of the analysis is 78.1% (*P. jaenensis* = 83.3%, *P. pusilla* = 75.9%, *P. rupestris* = 96.6%, and *P. saxatilis* = 66.7%). Type material for each species resides within the polygon demarcating that species location in 2-dimensional CVA space (fig. 4).

Landmark-based CVA shows analogous patterns with a higher overall classification accuracy of 90.9% (*P. jaenensis* = 93.3%, *P. pusilla* = 88.9%, *P. rupestris* = 96.6%, and *P. saxatilis* = 88.2%; fig. 5). Almost no overlap exists between *P. jaenensis* and *P. rupestris* and notably less between *P. pusilla* and *P. saxatilis*. Again, the type specimen for each species resides within the polygon demarcating that species (fig. 5).

Thin-plate splines, illustrating shape transitions between species pairs, show virtually no landmark shift between *P. pusilla* and *P. saxatilis* and only slight shifts in landmarks 1–5 between *P. rupestris* and *P. jaenensis* (fig. 5). These demarcate the apex and margin of the shell and indicate the tighter coiling of *P. jaenensis*. However, because landmark vectors range from very short to not apparent, high overall shell similarity is suggested. Because comparisons between high- and low-spined species yield virtually identical landmark vector shift patterns (supplementary fig. S4), for purposes of visualization we have only illustrated the comparison between these two groups.

In both, CVA based on traditional morphometrics and CVA based on landmarks, the first

two axes of the ordination account for > 90% of the variation in shell shape, with ~ 70% being explained by the first axis, reflecting the transition from low-spined towards high-spined morphotype.

Qualitative diagnostic features

High- and low-spined species possess consistent differences in apex / suture shape and growth ridge angle (table 2b). *Pyramidula jaenensis* and *P. rupestris* have highly convex whorls and deep suture, giving the impression of an almost flat upper whorl surface, especially in *P. jaenensis* (fig. 3). The apex of these species forms a twisted, well-pointed tip, and angle of growth ridges from the suture is less than ~ 45° (fig. 6a-b). In contrast, *P. pusilla* and *P. saxatilis* have relatively shallower, less tumid whorls, a flatter, less pronounced apex (fig. 3), and have the angle of growth ridges from the suture more than ~ 45° (fig. 6c-d).

The most important qualitative feature for species diagnosis is shell microsculpture (table 2b). Within the low-spined morphotypes, *P. saxatilis* possesses very fine and regular thread-like growth ridges (typically > 20 per 0.5 of shell surface), giving rather dull appearance to the shell (fig. 6c), whereas *P. pusilla* possesses much coarser and irregular growth ridges (< 14 per 0.5 mm) giving it a slightly shinier lustre (fig. 6d). A similar pattern is found in the high-spined morphotypes with *P. jaenensis* possessing fine, regular growth ridges (> 14 per 0.5 mm) and dull lustre (fig. 6a) and *P. rupestris* possessing coarse, irregular growth ridges (< 10 per 0.5 mm) and shiny lustre (fig. 6b). Type material of each species possesses these expected microsculpture traits. Combination of qualitative and quantitative shell features allows for the designation of lectotypes of *P. saxatilis* and *P. jaenensis* (fig. 7). Detailed descriptions of each species' distinguishing characters are given in table 2b and in *Taxonomic summary* below.



FIGURE 3 Variation in shell shape among genetically analyzed populations of four studied *Pyramidula* species; *P. jaenensis*: a) Jijona, Spain (P368); b) Venta del Moro, Spain (P376); c) Cazorla, Spain (P357); d) Gaeta, Italy (P210); e) Città di San Marino (P207); *P. rupestris*: a) Xàtiva, Spain (P374); b) Meyreuil, France (P373); c) Ollioules, France (P354); d) Encío, Spain (P366); e) Mura, Spain (P375); *P. saxatilis*: a) Nods, Switzerland (P229); b) Selva di Val Gardena, Italy (P249); c) Lunz am See, Austria (P231); d) Kamnik, Slovenia (P232); e) Hochschwab, Austria (P189); *P. pusilla*: a) Štramperk, Czech Republic; b) Johnsbach, Austria (P196); c) Liptovské Revúce, Slovakia (P369); d) Tatranská Kotlina, Slovakia (P213); e) Spital am Pyhrn, Austria (P193).

Traditional morphometrics and climate

The reduced set of seven uncorrelated climatic variables includes BIO1 = Annual Mean Temperature, BIO3 = Isothermality, BIO4 = Temperature Seasonality, BIO8 = Mean Temperature of Wettest Quarter, BIO14 = Precipitation of Driest Month, BIO15

= Precipitation Seasonality, and BIO19 = Precipitation of Coldest Quarter. Spearman correlations between these climatic variables and shell measurements range from -0.56 to 0.63, with only BIO1, BIO3, and BIO14 exceeding the rho coefficient value = |0.5| with at least one of the shell measurements (table 4).

TABLE 3 Multiple regressions of shell characteristics and specimen scores on the first two axes of the Canonical Variance Analysis. For details on the numbers of measured shells / populations see fig. 4

	CV1	CV2	R ²	P
Shell height	0.944	0.330	0.50	<0.001
Body height	0.946	-0.323	0.19	<0.001
Aperture height	0.834	-0.551	0.03	0.082
Shell width	-0.832	0.555	0.70	<0.001
Aperture width	0.031	1.000	0.03	0.080
No. of whorls	0.036	0.999	0.33	<0.001
Umbilicus width	-0.787	0.617	0.81	<0.001
Shell width / no. of whorls	-0.992	0.129	0.58	<0.001
Shell height / no. of whorls	0.984	-0.179	0.57	<0.001
Body height / shell height	-0.770	-0.638	0.77	<0.001
Aperture width / shell width	0.934	-0.357	0.54	<0.001
Aperture width / shell height	-0.999	-0.053	0.49	<0.001
Aperture height / body height	-0.984	0.179	0.21	<0.001
Shell height / shell width	0.995	-0.095	0.87	<0.001
Umbilicus width / no. of whorls	-0.850	0.526	0.76	<0.001

Abbreviations and symbols: CV1 and CV2, regression coefficients; R², fit of each characteristic into the ordination space, i.e., percentage variation explained by specimen scores on the first two CV axes in multiple linear regression; P, significance based on 4999 permutations.

In the linear regressions, the highest amount of explained variation is obtained for shell height / shell width in relation to BIO1 (Adj R² = 49.4%, $P < 0.001$; fig. 8). All observed significant relationships reflect the transition of low-spined / wide-umbilicus to high-spined / narrow-umbilicus shells towards areas with warmer climate with less precipitation (fig. 8). Shell volume does not change significantly with climate, suggesting that the observed changes in shell measurements are independent of overall shell size (table 4).

Taxonomic summary

Family *Pyramidulidae* Kennard et Woodward, 1914

Genus *Pyramidula* Fitzinger, 1833

Pyramidula Fitzinger, 1833: 95.

Type species. Helix rupestris Draparnaud, 1801, by monotypy (ICZN 0.335, 1987: 159).

Pyramidula pusilla (Vallot, 1801)

Helix pusilla Vallot, 1801: 5.

Type locality. France, Côte-d'Or, 'fontaine Ste. Anne' near Dijon. Neotype (fig. 7d) designated in Gittenberger & Bank (1996: 74).

Synonyms. *Pyramidula umbilicata* (Montagu, 1803), type locality: Wales, UK

Material examined. Thirteen populations from Austria, Czech Republic, Italy, and Slovakia.

Conchology. This species is characterized by low-spined shell, broader than wide, with wide umbilicus (typically 0.3 of the shell width), relatively shallow suture, and apical whorls rather blunt and gradually increasing in width. Shell color light- to dark reddish-brown in individuals with intact periostracum; older shells corrode towards greyish-blue color. Surface microsculpture is irregular, with frequent anastomose, growth ridges in a form of wrinkles and ribs, with smooth surfaces in between. Ridge density per 0.5 mm of teleoconch surface typically < 14, protoconch without structure. Angle of inclination of growth

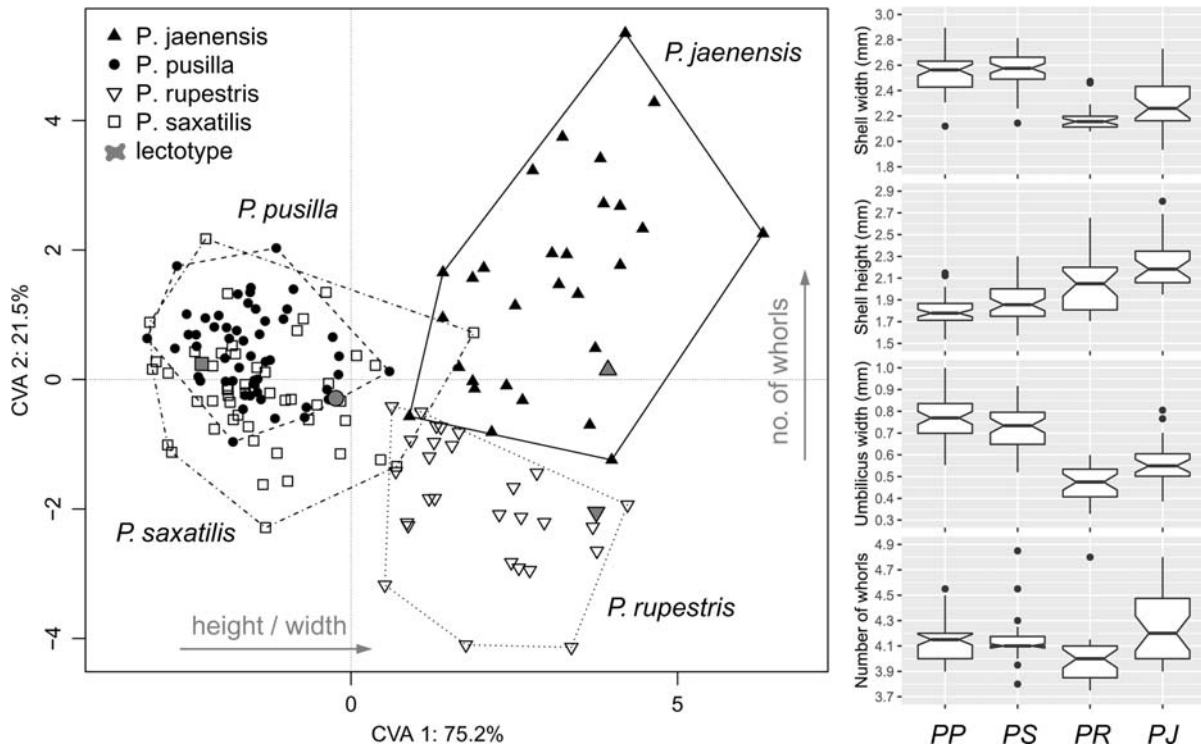


FIGURE 4 Position of measured shells along the first two axes of the Canonical Variance Analysis based on the fifteen measured shell parameters and their ratios (supplementary table S2). Numbers of measured shells / populations for each species: *P. jaenensis*: 29 / 7, *P. saxatilis*: 50 / 11, *P. rupestris*: 28 / 9, *P. pusilla*: 55 / 12. Convex polygons were added to the diagram to highlight the distinction between the four species. Type specimens of the respective species were also used in the analysis (see fig. 7 for details), and are shown in grey color. Variation in selected basic shell parameters among the four species (PP, *P. pusilla*; PS, *P. saxatilis*; PR, *P. rupestris*; PJ, *P. jaenensis*) is visualized using notched box-and-whisker plots on the right.

ridges right after the suture is always higher than 45° . There is a continuous variation from the phenotype described above, to populations that possess very low conical shells with widely open umbilicus (nearly 0.4 of the shell width). Shell shape is identical to that of *P. saxatilis*, which however possesses very distinct, thread-like surface microsculpture, with no irregularities (see details in the main text). *Pyramidula rupestris* and *P. jaenensis* differ in possessing high-spired shells, deep suture, narrow umbilicus, and inclination of growth ridges after the suture lower than 45° .

Biogeography. Reported by Razkin et al. (2017) from across temperate Europe and the Mediterranean, including British Isles, Iberian Peninsula, France, Italian Peninsula,

the Alps, Carpathians, Balkans, Anatolia, and Crimea. In this study reported also from lowlands and highlands in the Czech Republic and Slovakia.

Nomenclatural notes. The very low-spire form with widely open umbilicus has most likely led to the description of *P. umbilicata* (Montagu, 1803), which has been found identical with *P. pusilla* in the integrative analysis of Razkin et al. (2017).

Pyramidula saxatilis (Hartmann, 1842)
Delomphalus rupestris saxatilis Hartmann, 1842: 122.

Type locality. St. Georgen by St. Gallen, Switzerland. Lectotype (design. nov., fig. 7c): M562.1, Natural History Museum St. Gallen, Switzerland.

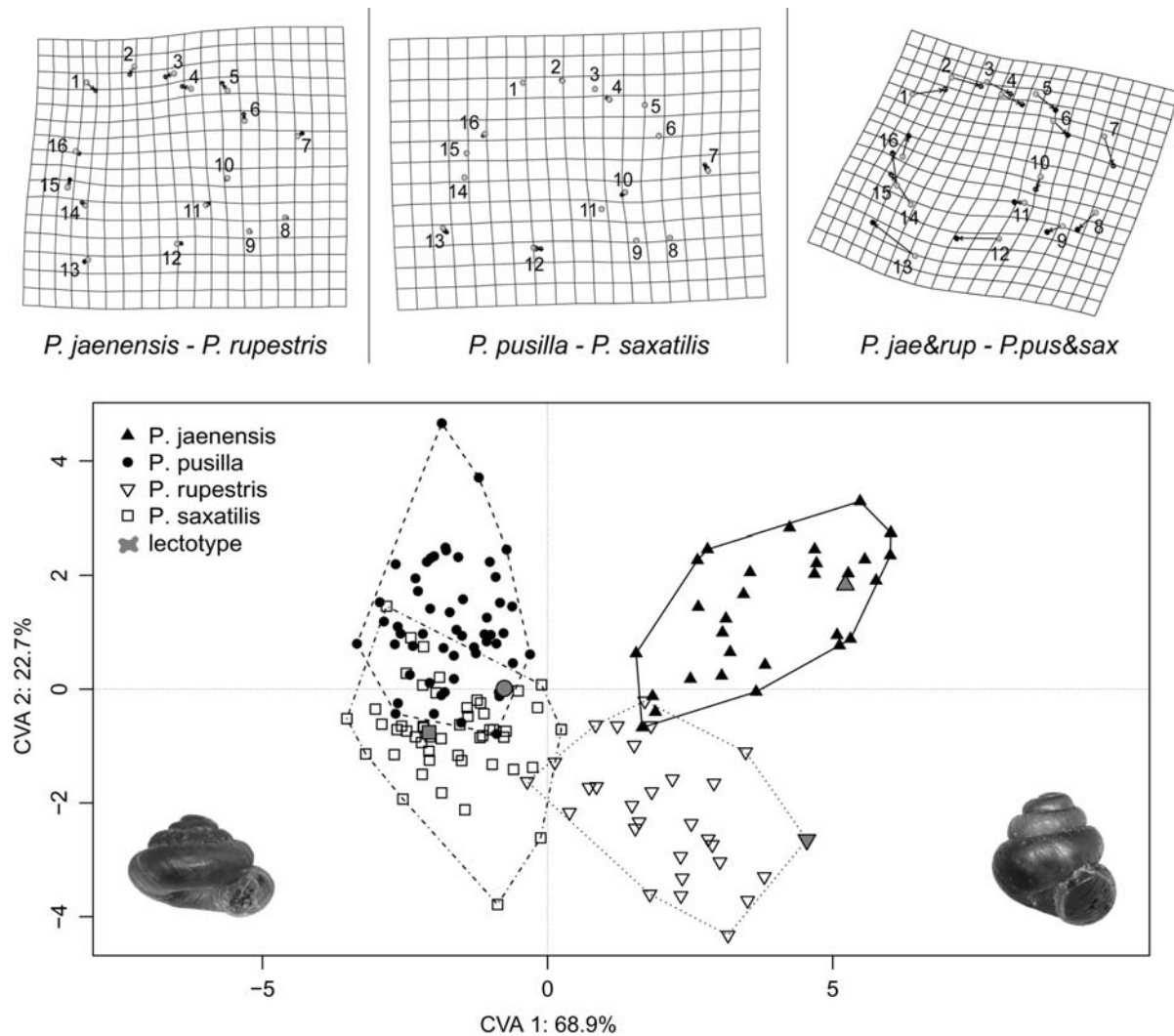


FIGURE 5 Result of geometric morphometrics using sixteen landmarks on the frontal shell view (supplementary fig. S2). Upper part: thin-plate splines, illustrating transitions in shape between pairs of species *P. jaenensis* and *P. rupestris*, and *P. pusilla* and *P. saxatilis*, and between the high-spired (former pair) and low-spired (latter pair) species combined. Lower part: Position of shells along the first two axes of the Canonical Variance Analysis (CVA1, CVA2) based on Procrustes shape coordinates of the landmark data. Convex polygons were added to the diagram to highlight the distinction between the four species. Type specimens of the respective species were also used in the analysis (see fig. 7 for details), and are shown in grey color.

Material examined. Seventeen populations from Austria, Italy, San Marino, Slovakia, and Switzerland.

Conchology. Shell low-spired, broader than wide, with wide umbilicus, shallow suture, blunt apex, and gradually increasing whorls; the variability of overall shell architecture overlaps highly with *P. pusilla*. However, it can be distinguished by very regular, dense,

thread-like microsculpture of fine but distinct growth ridges on the surface of entire shell, including body whorl. Ridge density per 0.5 mm of teleoconch surface typically > 20, protoconch without structure. In higher altitudes, e.g. in the Alps, it forms populations of very dark / black-colored shells. Some individuals of *P. saxatilis* possess relatively high spires when compared to the typical phenotype of

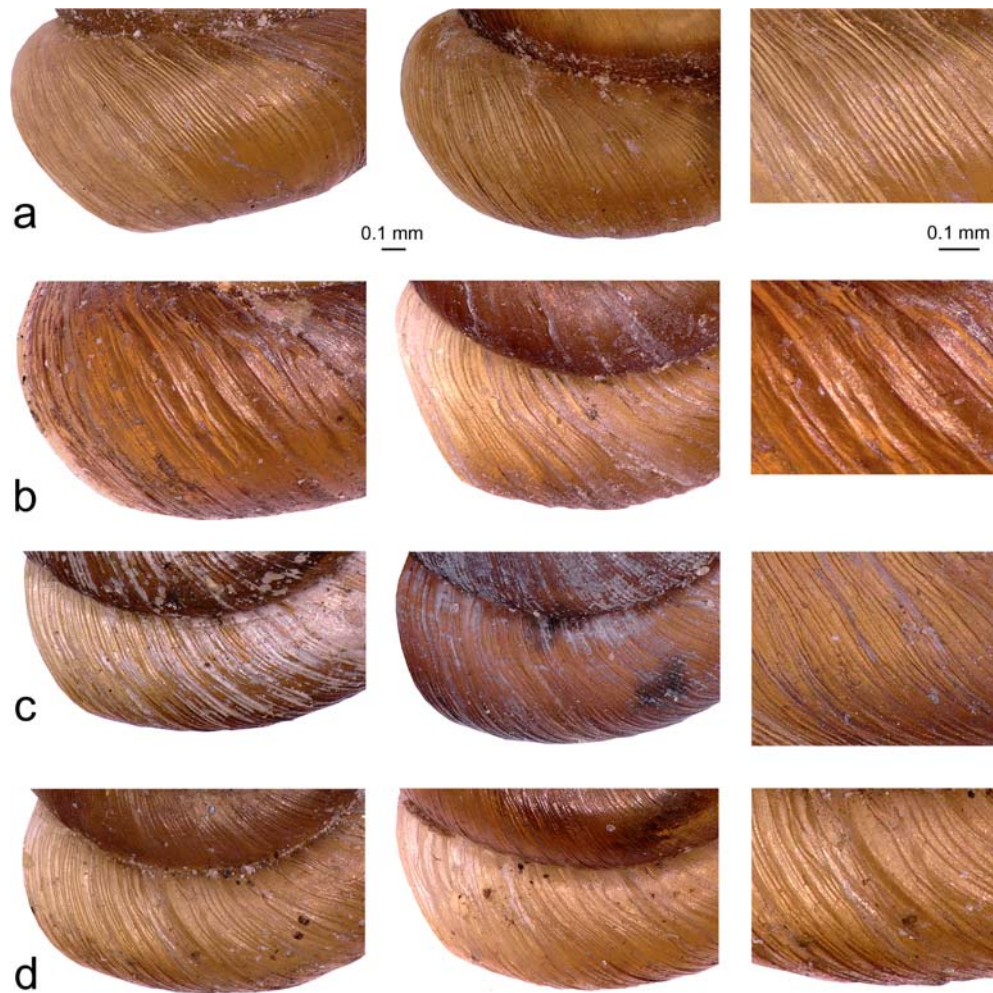


FIGURE 6 Upper face shell microsculpture on the last whorl in four *Pyramidula* species; a) *P. jaenensis* (from left to right): Jijona, Spain (P368), Città di San Marino (P207), P368; b) *P. rupestris*: Xàtiva, Spain (P374), Encio, Spain (P366), P374; c) *P. saxatilis*: Villeret, Switzerland (P208), Hochschwab, Austria (P189), P189; d) *P. pusilla*: Pavlov, Czech Republic (P211), Tatranská Kotlina, Slovakia (P213), P211. Scale bar: 0.1 mm.

this species (fig. 3e), thus resembling high-spired, narrow-umbilical *P. rupestris* and *P. jaenensis*. In such cases, it can be distinguished by shallower suture, more rounded apex, and inclination of growth ridges after the suture always higher than 45° .

Biogeography. Reported by Razkin et al. (2017) from the Alps, North Italian Peninsula, and one site in Slovakia. In this study reported also from NE Alps (numerous localities in Austria), Western Carpathians (several localities in Slovakia), Switzerland (incl. lectotype specimen), one locality in San Marino, and one in central Pyrenees (France).

Nomenclatural notes. Razkin et al. (2017) found that this species could be associated with the taxon first described as *Delomphalus rupestris saxatilis* by Hartmann (1842). However, the authors concluded: “We cannot designate a lectotype from the Hartmann material because it is not possible to doubtlessly identify a specimen belonging to *P. saxatilis*, based on shell morphology. Therefore, we will designate one of the specimens identified as *P. saxatilis* by DNA sequencing as neotype to stabilize the proposed usage of the name.” Based on the communication with the authors we found that the neotype designation

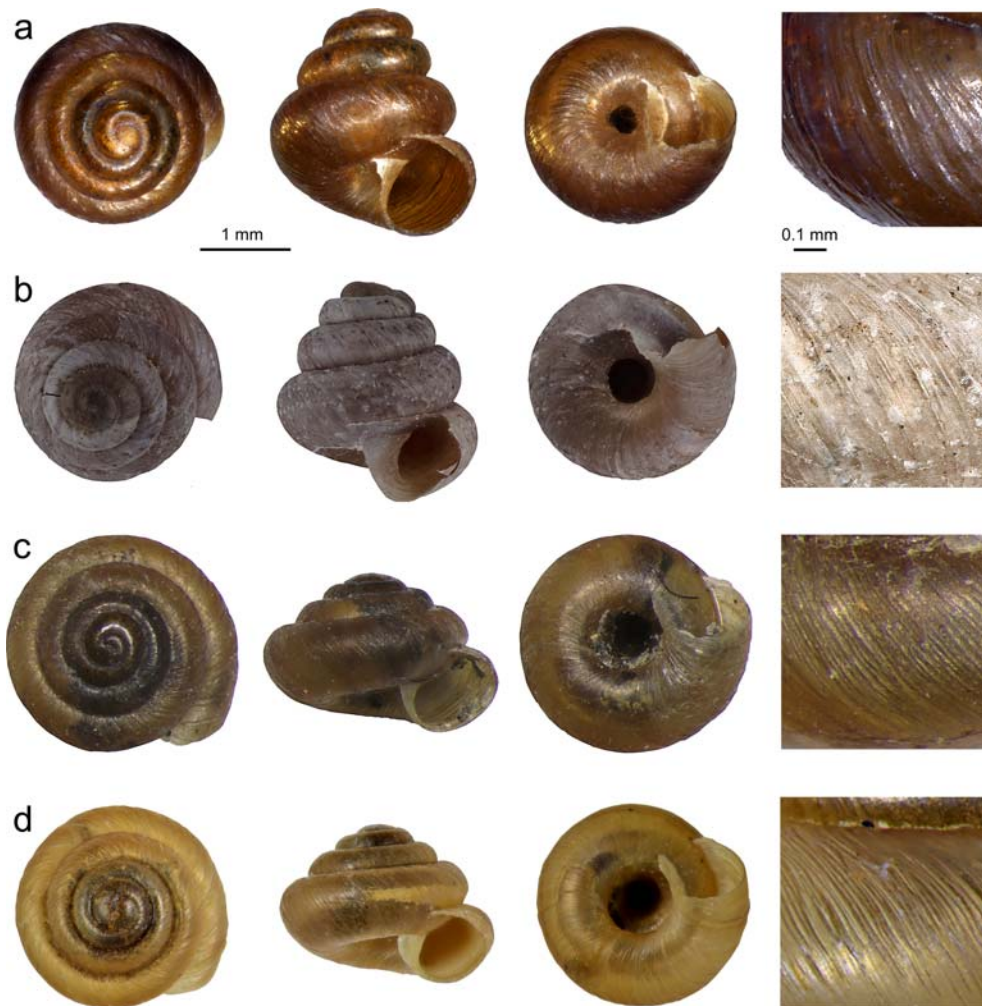


FIGURE 7 Type specimens of the four studied species: a) *Pyramidula jaenensis*, lectotype (design. nov.), collection of S. Clessin, no. SMNS-Z10142153, State Museum of Natural History Stuttgart, Germany. b) *P. rupestris*, lectotype, Draparnaud collection xxvi 97a, Natural History Museum, Vienna, Austria. c) *P. saxatilis* lectotype (design. nov.), collection of J. D. W. Hartmann, M562.1, Natural History Museum St. Gallen, Switzerland. d) *P. pusilla*, neotype, no. 210.996.MO.1, Natural History Museum, Dijon, France.

has not yet been conducted (A. Martínez-Ortí, pers. comm.). Further, with respect to newly discovered conchological features that allow for reliable identification of this species, as reported within the present study, we were able to acquire original material of Hartmann (stored at Natural History Museum St. Gallen, Switzerland), and designate the lectotype from the type series. The lectotype was selected from the sample lot containing > 100 individuals, collected at the rock outcrop near St. Georgen by St. Gallen (Switzerland). It was assigned no. M562.1 (fig. 7c). To verify our identification, we successfully extracted, amplified

and sequenced 603 bp of the cytochrome oxidase I gene from one individual of this > 170 years old material. In the phylogenetic reconstruction based on this marker alone, the individual fell among the individuals of *P. saxatilis* (supplementary fig. S3).

Pyramidula rupestris (Draparnaud, 1801)

Helix rupestris Draparnaud, 1801: 71.

Type locality. France. Lectotype (fig. 7b) designated in Gittenberger & Bank (1996: 76).

Material examined. Ten populations from France, Spain, and Switzerland.

Conchology. Shell high-spired, height similar to width, with pointed apex, very tumid

TABLE 4 Spearman correlations between climatic variables and measured shell parameters

	BIO1	BIO3	BIO14
Shell height	0.46***	0.50***	-0.51***
Body height	0.31**	0.39***	-0.34***
Aperture height	<i>0.16</i>	<i>0.12</i>	<i>-0.11</i>
Shell width	-0.41**	-0.46***	0.39***
Aperture width	<i>0.06</i>	<i>-0.07</i>	<i>-0.10</i>
No. of whorls	<i>-0.07</i>	<i>0.01</i>	<i>-0.05</i>
Umbilicus width	-0.48***	-0.56***	0.40***
Shell width / no. of whorls	-0.42**	-0.52***	0.42***
Shell height / no. of whorls	0.50***	0.54***	-0.51***
Body height / shell height	-0.52***	-0.40***	0.50***
Aperture width / shell width	0.47***	0.42***	-0.47***
Aperture width / shell height	-0.40***	-0.55***	0.40***
Aperture height / body height	-0.24**	-0.44***	0.32***
Shell height / shell width	0.54***	0.63***	-0.55***
Umbilicus width / no. of whorls	-0.47***	-0.57***	0.39***
Shell volume (mm ³)	-0.13	-0.16*	0.10

Abbreviations and symbols: BIO1, Annual Mean Temperature; BIO3, Isothermality; BIO14, Precipitation of Driest Month; *, P < 0.05; **, P < 0.01; ***, P < 0.001; bold, strongest correlation for each climatic variable; italics, variables not significant after Holm correction.

whorls with deep suture, relatively high coil expansion rate, resulting in high body whorl, and narrow umbilicus (ca 0.2 of the shell width). Shell color dark reddish-brown (in non-corroded individuals). Angle of inclination of growth ridges right after the suture is always lower than 45°. As in *P. pusilla*, surface microsculpture is coarse and irregular, with frequent anastomose (wrinkles and ribs). Ridge density per 0.5 mm of teleoconch surface typically < 10, protoconch with rugged structure. *Pyramidula pusilla* and *P. saxatilis* differ in possessing low-spired shells of wide umbilicus and shallow suture, lower coil expansion rate, inclination of growth ridges after the suture higher than 45°, and very regular thread-like growth ridges in the latter. Overall shell shape is very similar to *P. jaenensis*, which, however, can reach even more conical shape (height / width ratio often > 1) and possesses very regular, fine, thread-like surface microsculpture. *Pyramidula rupestris*

can occur in two relatively discrete forms: 1, fast growing shells with high body whorl, large aperture, very narrow umbilicus, and shiny lustre (fig. 3a-c, lectotype fig. 7b, microstructure fig. 6b left and right); 2, slightly flatter shells with lower body whorl, smaller aperture, wider umbilicus, and somewhat more regular and finer surface structure of dull appearance (fig. 3d-e, microstructure fig. 6b in the middle). This form can be hard to distinguish from some populations of *P. jaenensis*, which however possesses very regular growth ridges. In some cases this form can also resemble *P. saxatilis* and *P. pusilla*, in which case the inclination of growth ridges is informative. The identification of such individuals needs to be done with caution, using a suite of traits and ideally also genetic data. So far, there have been not enough data to explore which of the forms is more common, and whether the variation is related to any ecological, climatic, and geographical patterns.

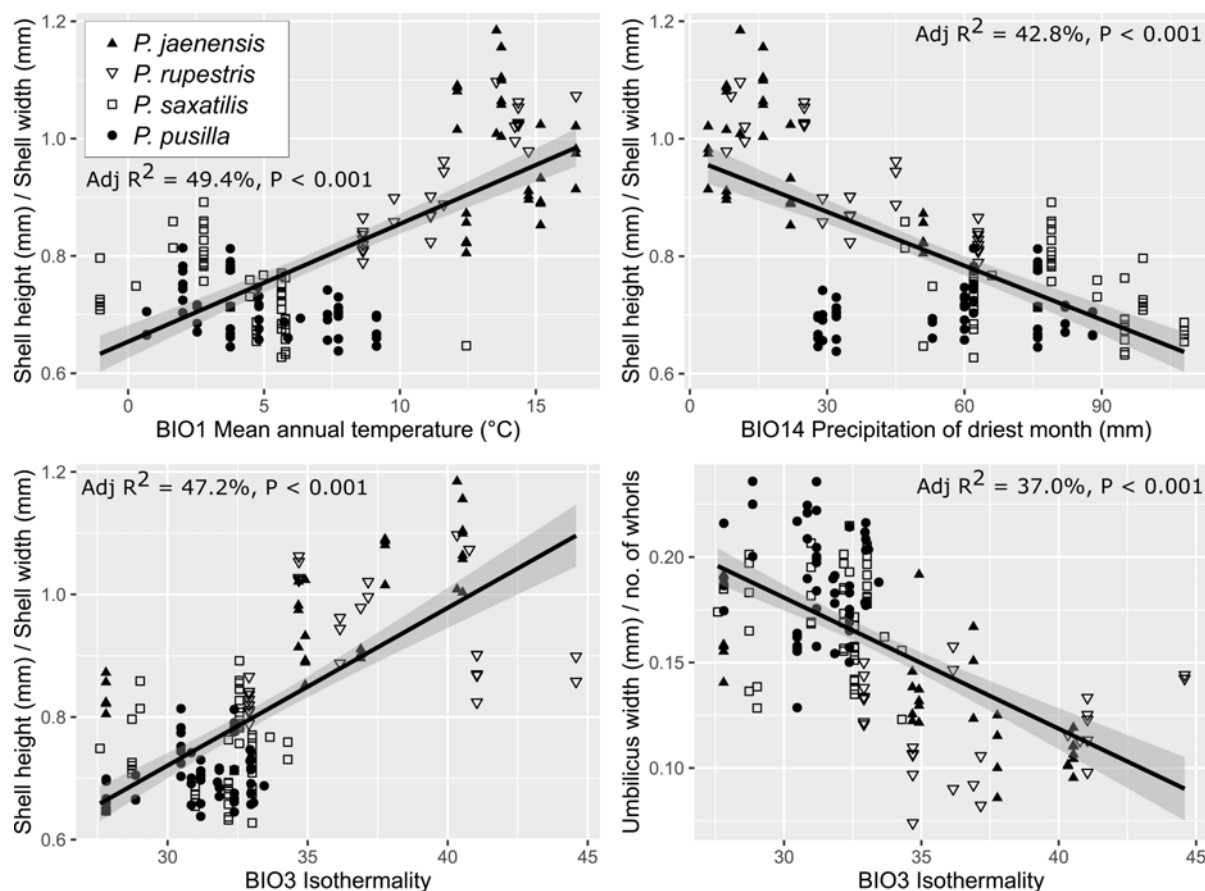


FIGURE 8 Linear regressions of selected shell parameters in relation to climatic variables inferred from the population locations. Regression lines, 95% confidence intervals, Adj R² values and P-values are shown.

Biogeography. Reported by Razkin et al. (2017) from the Iberian Peninsula and S France. In this study reported also from Switzerland and Italy (two populations that have not been genetically verified but clearly match all conchological criteria).

Pyramidula jaenensis (Clessin, 1882)

Helix (Patula) jaenensis Clessin, 1882: 187.

Type locality. Jaén, Andalusien, Spain. Lectotype (design. nov., fig. 7a): SMNS-ZI0142153, State Museum of Natural History, Stuttgart, Germany.

Material examined. Seven populations from France, Italy, San Marino, and Spain.

Conchology. Overall shell shape and architecture similar to *P. rupestris*, with high-spired, pointed apex, very tumid whorls with deep suture, slow coil expansion rate, high

body whorl, angle of inclination of growth ridges after the suture always lower than 45°, and narrow umbilicus. Shell height / width ratio often > 1, the whorls almost flattened on top along the suture. Shell color yellowish grey to dark brown, always of dull appearance (in non-corroded individuals). Ridge density per 0.5 mm of teleoconch surface typically > 14, protoconch with rugged structure. From *P. rupestris* it can be best distinguished by very regular, thread-like microsculpture of distinct growth ridges similar to *P. saxatilis* (which, however, possesses finer and denser ridges). *Pyramidula saxatilis* and *P. pusilla* differ in overall shell architecture of low-spired shells with wide umbilicus and shallow suture, inclination of growth ridges after the suture higher than 45°, and irregular coarse microsculpture

in the latter. Some populations reach nearly scalaroid shell shape, narrow umbilicus and tilted, pointed apex (fig. 3a-c), with the continuous variation towards populations of more depressed conical shape with shallower suture and wider umbilicus (fig. 3e-d).

Biogeography. Reported by Razkin et al. (2017) and Miller et al. (2021) from the Iberian Peninsula, N Africa, Menorca, Sicily, Sardinia, S France, Italy, Croatia, and Austria.

Nomenclatural notes. The type material of *P. jaenensis* has been considered lost. However, in the State Museum of Natural History, Stuttgart, Germany, a lot from the collection of S. Clessin was located, labelled as: “Andalusien, Jaén, Cerro de Albanoki, Clessin leg.,” which matches the localization in the original description of the species by Clessin (1882). This lot contains two specimens damaged by Byne’s disease, which can thus be considered syntypes of *P. jaenensis* (I. Richtling, pers. comm.). One of the specimens was less damaged and therefore designated as lectotype, and assigned no. SMNS-ZI0142153 (fig. 7a).

Discussion

Our sample set with more robust geographical coverage of the four studied Western Palearctic species (*Pyramidula jaenensis*, *P. rupestris*, *P. saxatilis*, and *P. pusilla*) is in agreement with the molecular phylogeny of Razkin et al. (2016, 2017). Where our analyses differ is in showing that each species exhibits a unique set of quantitative (shell height / width) and qualitative (fine / regular vs. coarse / irregular ribbing) features which in combination allow for accurate identification without consultation of DNA sequence. Based on our results the species of this study system can no longer be considered fully cryptic: if prior workers had been able to sort material into

biologically valid categories (i.e. evolutionarily independent species-level taxa) these features could have been observed. However, without access to DNA sequence data the profound overlap between taxa in simple height vs. width space made such sorting impossible. This work should thus serve as a reminder that DNA sequence data should be used to place material into their correct biological categories *before* identification criteria are sought, and that “cryptic” species might nevertheless be morphologically differentiated.

Our study also emphasizes the potential importance of subtle qualitative shell sculpture and architecture traits in identifying species. In *Pyramidula*, these traits in conjunction with shell height / width and whorl expansion ratios are essential for accurate visual species assignment. Although other integrative taxonomic revisions have also shown the utility of shell microsculpture in accurate species demarcation (e.g., Elejalde et al., 2008; Nekola et al., 2015, 2018; Horsáková et al., 2019), more focus has traditionally placed on macroscopic features such as shell color, calcification, aperture lamellae, and size which are more susceptible to adaptation (e.g., Emberton, 1995; Chiba & Davison, 2007; Elejalde et al., 2008; Horsáková et al., 2019; Köhler et al., 2020) and thus less likely to provide a clear taxonomic signal (e.g., Goodfriend, 1986; Cameron, 2016).

Univariate vs. multivariate morphometrics

This work also clearly shows the importance of considering morphometrics within a multivariate context. Razkin et al. (2016, 2017) previously only compared ratios of shell height and umbilicus width vs. shell width, showing that these metrics overlap to a certain degree among all four species within our study system. We considered seven different single variables, eight different compound variables, along with 16 different shell landmarks. Unlike simple measurement ratios, multivariate

analyses demonstrated that *P. pusilla* / *saxatilis* can be distinguished from *P. jaenensis* / *rupestris*, and *P. jaenensis* from *P. rupestris*. However, without use of multivariate CVA these distinctions were lost within a sea of low-dimensional intraspecific variability.

Although CVA worked reasonably well on the 15 measured shell traits, the results were even more precise when using 16 landmarks, with overall classification accuracy exceeding 90% and with there being a relatively low degree of overlap between even *P. pusilla* and *P. saxatilis*. The advantages of landmark analysis have been previously highlighted in many malacological studies (e.g., Schilthuizen & Haase, 2010; Haase et al., 2013; Giokas et al., 2014), as it allows for shell shape to be analyzed independent of size, rotation of the shell, and allometry (Rohlf & Marcus, 1993; Webster & Sheets, 2010; Dillon & Jacquemin, 2015). While more time consuming, this method appears to capture more quantitative information be superior to traditional multivariate morphometrics (Stone, 1998; Conde-Padín et al., 2007; Dillon & Jacquemin, 2015; Gladstone, 2019). However, landmark analysis may have less value in determining environmental drivers underlying shell variation, as these analyses are easier to interpret when based on specific non-point shell characters like height and width.

Our results partially agree with those of Miller et al. (2021) who focused on *P. jaenensis* and *P. rupestris*, and demonstrated a distinction between these species in landmark-based PCA. Their study, however, did not fully encompass morphological variation of these species, because of a small sample size and limited geographical coverage (only two *P. jaenensis* populations from Spain were analyzed). The constrained variation of their data was probably the reason why the authors observed a clear separation even using PCA analysis, which does not incorporate *a priori*

group assignments. In our study, only CVA – maximizing the separation between pre-defined groups – showed limited overlap between the two species while PCA did not (supplementary fig. S5).

Adaptive shell shape traits

The conchological similarity between the polyphyletic *P. saxatilis* / *pusilla* and *P. jaenensis* / *rupestris* groups suggests that adaptive evolutionary processes have actively altered shell dimensions. What mechanisms may be responsible for this? Although low vs. high-spired land snail shells have been previously claimed to be associated with horizontal vs. vertical habitats (Cain, 1977; Teshima et al., 2003; Elejalde et al., 2008; Haase et al., 2013), such explanations are not relevant for these *Pyramidula* which all reside on largely bare, vertical, open, base-rich rocks. And when they do co-occur they often occupy the same 10 cm² microsites. As suggested by Razkin et al. (2017), our analyses confirm that conchological variation in *Pyramidula* is more related to meso-scale climate, with low-spired shells being more common in cooler regions with higher precipitation and high-spired shells more common in warmer regions with lower precipitation.

It is always challenging to prove causal links between morphological traits and environmental factors (Goodfriend, 1986; Davison, 2002). However, as land snails are very sensitive to desiccation, many adaptive shell modifications likely target the heat and water budget (Cook, 2001; Pfenninger et al., 2005; Giokas et al., 2014) especially in dry environments and/or arid climates (Giokas et al., 2005). In colder climates, traits/behaviors often evolve to mitigate tissue freezing (Ansart & Vernon, 2003; Schamp et al., 2010).

In ectothermic organisms, body temperature is primarily controlled by substratum temperature (Chappon & Seuront, 2011). Rock outcrop temperatures are primarily

driven by solar irradiance (Marshall et al., 2010), allowing them to often be higher than adjacent shaded air temperature (Jenkins & Smith, 1990; Molaro & McKay, 2010). We thus suggest that for *Pyramidula* species rock surface temperature might represent a key selection factor: given a uniform shell volume, higher shells will minimize the substrate / body interface and increase heat flux into the atmosphere. This could be important in warmer climates where rock surfaces are more likely to become lethally hot. In contrast, flatter shells will maximize the substrate / body interface and minimize heat flux away from the body. This could be advantageous in cold-climate regions where proximity to relatively warmer rock surfaces might provide sparing from freezing.

We emphasize that we have not directly tested this mechanism and that these ideas should be simply taken as informed conjecture to explain why *Pyramidula* shell shapes appear more related to regional climate than evolutionary similarity. Clearly additional experimental work will be required to assess the plausibility of this hypothesis.

How to approach “cryptic” species complexes?

This study stresses the importance of detailed *post-hoc* analyses combining multiple types of data as a follow-up for initial “cryptic” species discoveries. As well as integrative studies of other micro-gastropods (e.g., Weigand et al., 2012; Nekola et al., 2015, 2018; Horsáková et al., 2019) we illustrate that presumed species crypticity must be carefully reevaluated, given that most biologically valid species possess some suite of robust visually-observable diagnostic characters. The issue is in separating such robust traits from those which are misleading in isolation or which possess too much plasticity to allow for accurate identification.

We suggest the following order-of-operations which if followed should achieve this goal. First, it is essential to accumulate an ample sample sourced from across the known biogeographic and ecological range of all traditionally recognized taxonomic units within the study system. Second, this material should be subjected to a thorough phylogenetic analysis based on separate consideration of quasi-independent mtDNA and nDNA sequences. Of course, multiple nDNA regions would preferentially be separately analyzed across different linkage groups (Nekola et al., 2018); however this is hardly possible in land snails due to dearth of appropriate nDNA targets providing species-level information. Third, using consensus across these DNA signals, biologically valid groups are identified. Lastly, specimens from these groups are then sorted together, with their shells being critically evaluated for robust traits. Some of these, like shell microsculpture, may initially appear to be trivial. However, these may provide more reliable signal than more easily observed features. This is analogous to the centuries old “Morrelian method” of art historians, which seeks to identify a painter not through the “most obvious characteristics” but rather by “concentrate[ing] on minor details, especially those least significant in the style typical of the painter’s own school” (Ginzburg & Davin, 1980).

Ideally, this protocol should result in documentation of robust macroscale identification features which correspond to phylogenetic reconstructions. In empirically validating which visible factors are reliable in species-scale identification, future workers will be able to accurately identify material without need of DNA sequence data. Such morphology-based identification is crucial for gathering large datasets required to precisely document ecological and biodiversity patterns, and optimize conservation priorities

(Beheregaray & Caccone, 2007; Schlick-Steiner et al., 2007).

Acknowledgements

We are very thankful to K. Urfer, E. Fara, S. Puissant, I. Gallmetzer, D. Wanke, M. Pallmann, I. Richtling, S. Hof, E. Gittenberger, E. Schwabe for consultations, museum loans and / or help with imaging and measurements of type material; R. Coufal provided additional material of *P. saxatilis*. The study was primarily funded by the Czech Science Foundation (GA20-18827S). Eike Neubert (Naturhistorisches Museum Bern) and two anonymous referees gave valuable advice on the manuscript during the review process.

Supplementary material

Supplementary material is available online at: <https://doi.org/10.6084/m9.figshare.19582105>

References

- Adams, D.C., Collyer, M.L., Kaliontzopoulou, A. & Baken, E. (2021) *Geomorph: Software for geometric morphometric analyses*. R Package Version 3.3.2.
- Ansart, A. & Vernon, P. (2003) Cold hardiness in molluscs. *Acta Oecol.*, 24, 95–102.
- Armbruster, G.F. & Bernhard, D. (2000) Taxonomic significance of ribosomal ITS-1 sequence markers in self-fertilizing land snails of *Cochlicopa* (Stylommatophora, Cochlicopidae). *Zoosystematics Evol.*, 76, 11–18.
- Baker, R.J. & Bradley, R.D. (2006) Speciation in mammals and the genetic species concept. *J. Mammal.*, 87, 643–662.
- Balashov, I.A. & Gural-Sverlova, N.V. (2011) Terrestrial molluscs of the genus *Pyramidula* (Pyramidulidae, Pulmonata, Gastropoda) in the East Europe, Central Asia and adjacent territories. *Zool. Zhurnal.*, 90, 1423–1430.
- Beheregaray, L.B. & Caccone, A. (2007) Cryptic biodiversity in a changing world. *J. Biol.*, 6, 9.
- Bickford, D., Lohman, D.J., Sodhi, N.S., Ng, P.K., Meier, R., Winker, K., et al. (2007) Cryptic species as a window on diversity and conservation. *Trends Ecol. Evol.*, 22, 148–155.
- Cain, A.J. (1977) Variation in the spire index of some coiled gastropod shells and its evolutionary significance. *Philos. Trans. R. Soc. B.*, 277, 377–428.
- Cameron, R. (2003) *Land snails in the British Isles*. Field Studies Council, Shropshire.
- Cameron, R. (2016) *Slugs and snails*. HarperCollins Publishers, London.
- Chappon, C. & Seuront, L. (2011) Space–time variability in environmental thermal properties and snail thermoregulatory behaviour. *Funct. Ecol.*, 25, 1040–1050.
- Chiba, S. & Davison, A. (2007) Shell shape and habitat use in the North-west Pacific land snail *Mandarina polita* from Hahajima, Ogasawara: current adaptation or ghost of species past? *Biol. J. Linn. Soc.*, 91, 149–159.
- Conde-Padín, P., Grahame, J.W. & Rolán-Alvarez, E. (2007) Detecting shape differences in species of the *Littorina saxatilis* complex by morphometric analysis. *J. Molluscan Stud.*, 73, 147–154.
- Cook, A. (2001) Behavioural ecology: on doing the right thing, in the right place at the right time. In: G.M. Barker (Ed) *The biology of terrestrial molluscs*, pp. 447–487. CABI Publishing, New York.
- Darriba, D., Taboada, G.L., Doallo, R. & Posada, D. (2012) jModelTest 2: more models, new heuristics and parallel computing. *Nat. Methods*, 9, 772.
- Davison, A. (2002) Land snails as a model to understand the role of history and selection in the origins of biodiversity. *Popul. Ecol.*, 44, 129–136.
- Dayrat, B. (2005) Towards integrative taxonomy. *Biol. J. Linn. Soc.*, 85, 407–417.

- De Queiroz, K. (2007) Species concepts and species delimitation. *Syst. Biol.*, 56, 879–886.
- Dillon, Jr R.T. & Jacquemin, S.J. (2015) The heritability of shell morphometrics in the freshwater pulmonate gastropod *Physa*. *PLoS One*, 10:e0121962.
- Dray, S. & Dufour, A. (2007) The ade4 Package: Implementing the duality diagram for ecologists. *J. Stat. Softw.*, 22, 1–20.
- Drummond, A.J. & Rambaut, A. (2007) BEAST: Bayesian evolutionary analysis by sampling trees. *BMC Evol. Biol.*, 7, 214.
- Elejalde, M.A., Madeira, M.J., Arrebola, J.R., Munoz, B. & Gómez-Moliner, B.J. (2008) Molecular phylogeny, taxonomy and evolution of the land snail genus *Iberus* (Pulmonata: Helicidae). *J. Zoolog. Syst. Evol. Res.*, 46, 193–202.
- Emberton, K.C. (1995) Sympatric convergence and environmental correlation between two land-snail species. *Evolution*, 49, 469–475.
- ESRI. (2003) ArcGIS 8.3. Environmental Systems Research Institute, Redlands, CA, USA. Available from <http://www.esri.com> [Accessed 10 Sept 2021].
- Felsenstein, J. (1985) Confidence limits on phylogenies: an approach using the bootstrap. *Evolution*, 39, 783–791.
- Fišer, C., Robinson, C.T. & Malard, F. (2018) Cryptic species as a window into the paradigm shift of the species concept. *Mol. Ecol.*, 27, 613–635.
- Fisher-Reid, M.C. & Wiens, J.J. (2011) What are the consequences of combining nuclear and mitochondrial data for phylogenetic analysis? Lessons from *Plethodon* salamanders and 13 other vertebrate clades. *BMC Evol. Biol.*, 11, 1–20.
- Ginzburg, C. & Davin, A. (1980) Morelli, Freud and Sherlock Holmes: clues and scientific method. *Hist. Workshop*, 9, 5–36.
- Giokas, S., Pafilis, P. & Valakos, E. (2005) Ecological and physiological adaptations of the land snail *Albinaria caerulea* (Pulmonata: Clausiliidae). *J. Molluscan Stud.*, 71, 15–23.
- Giokas, S., Páll-Gergely, B. & Mettouris, O. (2014) Nonrandom variation of morphological traits across environmental gradients in a land snail. *Evol. Ecol.*, 28, 323–340.
- Gittenberger, E. & Bank, R.A. (1996) A new start in *Pyramidula* (Gastropoda Pulmonata: Pyramidulidae). *Basteria*, 60, 71–78.
- Gladstone, N.S. (2019) Morphometrics and phylogeography of the cave-obligate land snail *Helicodiscus barri* (Gastropoda, Stylommatophora, Helicodiscidae). *Subterr. Biol.*, 30, 1–32.
- Goodfriend, G.A. (1986) Variation in land-snail shell form and size and its causes: a review. *Syst. Biol.*, 35, 204–223.
- Gower, J.C. (1975) Generalized procrustes analysis. *Psychometrika*, 40, 33–51.
- Haase, M., Esch, S. & Misof, B. (2013) Local adaptation, refugial isolation and secondary contact of Alpine populations of the land snail *Arianta arbustorum*. *J. Molluscan Stud.*, 79, 241–248.
- Heethoff, M. (2018) Cryptic species—conceptual or terminological chaos? A response to Struck et al. *Trends Ecol. Evol.*, 33, 310.
- Hijmans, R.J., Cameron, S.E., Parra, J.L., Jones, P.G. & Jarvis, A. (2005) Very high resolution interpolated climate surfaces for global land areas. *Int. J. Climatol.*, 25, 1965–1978.
- Hinojosa, J.C., Koubínová, D., Szenteczki, M.A., Pitteloud, C., Dincă, V., Alvarez, N. & Vila, R. (2019) A mirage of cryptic species: genomics uncover striking mitonuclear discordance in the butterfly *Thymelicus sylvestris*. *Mol. Ecol.*, 28, 3857–3868.
- Holm, S. (1979) A simple sequentially rejective multiple test procedure. *Scand. J. Stat.*, 6, 65–70.
- Horsák, M. & Meng, S. (2018) *Punctum lozeki* n. sp. – a new minute land-snail species (Gastropoda: Punctidae) from Siberia and Alaska. *Malacologia*, 62, 11–20.
- Horsáková, V., Nekola, J.C. & Horsák, M. (2019) When is a “cryptic” species not a cryptic species: A consideration from the Holarctic micro-landsnail genus *Euconulus* (Gastropoda:

- Stylommatophora). *Mol. Phylogenet. Evol.*, 132, 307–320.
- Huelsenbeck, J.P. & Ronquist, F. (2001) MRBAYES: Bayesian inference of phylogenetic trees. *Bioinformatics*, 17, 754–755.
- Jenkins, K.A. & Smith, B.J. (1990) Daytime rock surface temperature variability and its implications for mechanical rock weathering: Tenerife, Canary Islands. *Catena*, 174, 449–459.
- Jörger, K.M. & Schrödl, M. (2013) How to describe a cryptic species? Practical challenges of molecular taxonomy. *Front. Zool.*, 10, 1–27.
- Karanovic, T., Djurakic, M. & Eberhard, S.M. (2016) Cryptic species or inadequate taxonomy? Implementation of 2D geometric morphometrics based on integumental organs as landmarks for delimitation and description of copepod taxa. *Syst. Biol.*, 65, 304–327.
- Katoh, K. & Toh, H. (2008) Improved accuracy of multiple ncRNA alignment by incorporating structural information into a MAFFT-based framework. *BMC Bioinform.*, 9, 1–13.
- Katoh, K., Rozewicki, J. & Yamada, K.D. (2019) MAFFT online service: multiple sequence alignment, interactive sequence choice and visualization. *Brief Bioinformatics*, 20, 1160–1166.
- Kerney, M.P. & Cameron, R.A.D. (1979) *Field guide to the land snails of Britain and north-west Europe*. Collins, UK.
- Klemm, W. (1974) *Die Verbreitung der rezenten Land-Gehäuse-Schnecken in Österreich*. Springer, Wien.
- Köhler, F., Criscione, F., Hallan, A., Hyman, I. & Kessner, V. (2020) Lessons from Timor: Shells are poor taxonomic indicators in *Asperitas* land snails (Stylommatophora, Dyakiidae). *Zool. Scr.*, 49, 732–745.
- Kuraku, S., Zmasek, C.M., Nishimura, O. & Katoh, K. (2013) aLeaves facilitates on-demand exploration of metazoan gene family trees on MAFFT sequence alignment server with enhanced interactivity. *Nucleic Acids Res.*, 41, W22–W28.
- Letunic, I. & Bork, P. (2021) Interactive Tree Of Life (iTOL) v5: an online tool for phylogenetic tree display and annotation. *Nucleic Acids Res.*, 49, W293–W296.
- Marshall, D.J., McQuaid, C.D. & Williams, G.A. (2010) Non-climatic thermal adaptation: implications for species' responses to climate warming. *Biol. Lett.*, 6, 669–673.
- Martínez-Ortí, A., Gómez-Moliner, B.J. & Prieto, C.E. (2007) El género *Pyramidula* Fitzinger 1833 (Gastropoda, Pulmonata) en la Península Ibérica. *Iberus*, 25, 77–87.
- Mayden, R.L. (1997) A hierarchy of species concepts: the denouement in the saga of the species problem. In: M.F. Claridge, H.A. Dawah & M.R. Wilson (Eds) *Species: The units of diversity*, pp. 381–423. Chapman & Hall, New York.
- Mayr, E. (2000) The biological species concept. In: Q.D. Wheeler & R. Meier (Eds) *Species concepts and phylogenetic theory: a debate*, pp. 17–29. Columbia University, New York Press.
- Miller, J.P., García-Guerrero, F., Rodríguez Sousa, A.A. & Carrillo Pacheco, M. (2021) Taxonomic redefining of *Pyramidula jaenensis* (Clessin, 1882) (Gastropoda: Pyramidulidae) based on an integrative taxonomy approach. *Invertebr. Zool.*, 18, 465–480.
- Molaro, J.L. & McKay, C.P. (2010) Processes controlling rapid temperature variations on rock surfaces. *Earth Surf. Process. Landf.*, 35, 501–507.
- Nekola, J.C., Coles, B.F. & Bergthorsson, U. (2009) Evolutionary pattern and process within the *Vertigo gouldii* (Mollusca: Pulmonata, Pupillidae) group of minute North American land snails. *Mol. Phylogenet. Evol.*, 53, 1010–1024.
- Nekola, J.C., Coles, B.F. & Horsák, M. (2015) Species assignment in *Pupilla* (Gastropoda: Pulmonata: Pupillidae): integration of DNA-sequence data and conchology. *J. Molluscan Stud.*, 81, 196–216.
- Nekola, J.C., Chiba, S., Coles, B.F., Drost, C.A., von Proschwitz, T. & Horsák, M. (2018) A phylogenetic overview of the genus *Vertigo*

- O. F. Müller, 1773 (Gastropoda: Pulmonata: Pupillidae: Vertigininae). *Malacologia*, 62, 21–161.
- Oksanen, J., Blanchet, F.G., Friendly, M., Kindt, R., Legendre, P., McGlinn, D., et al. (2017) “vegan: Community Ecology Package”. R Package Version 2.4–3.
- Padial, J.M., Miralles, A., De la Riva, I. & Vences, M. (2010) The integrative future of taxonomy. *Front. Zool.*, 7, 1–14.
- Pfenninger, M., Hrabakova, M., Steinke, D. & Depraz, A. (2005) Why do snails have hairs? A Bayesian inference of character evolution. *BMC Evol. Biol.*, 5, 59.
- Pilsbry, H.A. & Hirase, Y. (1902) Notices of new Japanese land snails. *The Nautilus*, 16, 75–80.
- Pokryszko, B.M., Auffenberg, K., Hlaváč, J.Č. & Naggs, F. (2009) Pupilloidea of Pakistan (Gastropoda: pulmonata): Truncatellinae, Vertigininae, Gastrocoptinae, Pupillinae (In Part). *Annal. Zool.*, 59, 423–458.
- Razkin, O., Sonet, G., Breugelmanns, K., Madeira, M.J., Gómez-Moliner, B.J. & Backeljau, T. (2016) Species limits, interspecific hybridization and phylogeny in the cryptic land snail complex *Pyramidula*: the power of RADseq data. *Mol. Phylogenet Evol.*, 101, 267–278.
- Razkin, O., Gómez-Moliner, B.J., Vardinoyannis, K., Martínez-Ortí, A. & Madeira, M.J. (2017) Species delimitation for cryptic species complexes: case study of *Pyramidula* (Gastropoda, Pulmonata). *Zool. Scr.*, 46, 55–72.
- Rohlf, F.J. & Marcus, L.F. (1993) A revolution morphometrics. *Trends Ecol. Evol.*, 8, 129–132.
- Rubinoff, D., Cameron, S. & Will, K. (2006) A genomic perspective on the shortcomings of mitochondrial DNA for “barcoding” identification. *J. Hered.*, 97, 581–594.
- Sáez, A.G. & Lozano, E. (2005) Body doubles. *Nature*, 433, 111.
- Schamp, B., Horsák, M. & Hájek, M. (2010) Deterministic assembly of land snail communities according to species size and diet. *J. Anim. Ecol.*, 79, 803–810.
- Schileyko, A.A. & Balashov, I.A. (2012) *Pyramidula kuznetsovi* sp. nov. – a new species of land molluscs from Nepal (Pulmonata, Pyramidulidae). *Ruthenica*, 22, 41–45.
- Schilthuizen, M. & Haase, M. (2010) Disentangling true shape differences and experimenter bias: are dextral and sinistral snail shells exact mirror images? *J. Zool.*, 282, 191–200.
- Schlager, S. (2017) Morpho and Rvcg – Shape Analysis in R. In: G. Zheng, S. Li, G. Székely (Eds) *Statistical Shape and Deformation Analysis*, pp. 217–256. Academic Press.
- Schlesinger, M.D., Feinberg, J.A., Nazdrowicz, N.H., Kleopfer, J.D., Beane, J.C., Bunnell, J.F. et al. (2018) Follow-up ecological studies for cryptic species discoveries: Decrypting the leopard frogs of the eastern US. *PLoS One*, 13, e0205805.
- Schlick-Steiner, B.C., Seifert, B., Stauffer, C., Christian, E., Crozier, R.H. & Steiner, F.M. (2007) Without morphology, cryptic species stay in taxonomic crypsis following discovery. *Trends Ecol. Evol.*, 22, 391–392.
- Schlick-Steiner, B.C., Steiner, F.M., Seifert, B., Stauffer, C., Christian, E. & Crozier, R.H. (2010) Integrative taxonomy: a multisource approach to exploring biodiversity. *Annu. Rev. Entomol.*, 55, 421–438.
- Stamatakis, A. (2014) RAxML Version 8: A tool for phylogenetic analysis and post-analysis of large phylogenies. *Bioinformatics*, 30, 1312–3.
- Stone, J. (1998) Landmark-based thin-plate spline relative warp analysis of gastropod shells. *Syst. Biol.*, 47, 254–263.
- Struck, T.H., Feder, J.L., Bendiksbj, M., Birkeland, S., Cerca, J., Gusarov, V.I. et al. (2018) Finding evolutionary processes hidden in cryptic species. *Trends Ecol. Evol.*, 33, 153–163.
- Tamura, K., Stecher, G., Peterson, D., Filipiński, A. & Kumar, S. (2013) MEGA6: molecular evolutionary genetics analysis version 6.0. *Mol. Biol. Evol.*, 30, 2725–2729.
- Tan, D.S., Ang, Y., Lim, G.S., Ismail, M.R.B. & Meier R. (2010) From ‘cryptic species’ to integrative taxonomy: an iterative process involving

- DNA sequences, morphology, and behaviour leads to the resurrection of *Sepsis pyrrhosoma* (Sepsidae: Diptera). *Zool. Scr.* 39, 51–61.
- Teshima, H., Davison, A., Kuwahara, Y., Yokoyama, J., Chiba, S., Fukuda, T. et al. (2003) The evolution of extreme shell shape variation in the land snail *Ainohelix editha*: a phylogeny and hybrid zone analysis. *Mol. Ecol.*, 12, 1869–1878.
- Valdecasas, A.G., Williams, D. & Wheeler, Q.D. (2008) 'Integrative taxonomy' then and now: a response to Dayrat (2005). *Biol. J. Linn. Soc.*, 93, 211–216.
- Wade, C.M. & Mordan, P.B. (2000) Evolution within the gastropod molluscs; using the ribosomal RNA gene-cluster as an indicator of phylogenetic relationships. *J. Molluscan Stud.*, 66, 565–569.
- Webster, M.A.R.K. & Sheets, H.D. (2010) A practical introduction to landmark-based geometric morphometrics. *Paleontol. Soc. Pap.*, 16, 163–188.
- Weigand, A.M., Götze, M.C. & Jochum, A. (2012) Outdated but established?! Conchologically driven species delineations in microgastropods (Carychiidae, *Carychium*). *Org. Divers. Evol.*, 12, 377–386.
- Welter-Schultes, F.W. (2012) *European non-marine molluscs, a guide for species identification*. Planet Poster Editions, Göttingen.
- Wickham, H. (2016) *ggplot2: Elegant Graphics for Data Analysis*. Springer-Verlag, New York.
- Wiens, J.J., Kuczynski, C.A. & Stephens, P.R. (2010) Discordant mitochondrial and nuclear gene phylogenies in emydid turtles: implications for speciation and conservation. *Biol. J. Linn. Soc.*, 99, 445–461.
- Will, K.W., Mishler, B.D. & Wheeler, Q.D. (2005) The perils of DNA barcoding and the need for integrative taxonomy. *Syst. Biol.*, 54, 844–851.